Title	S-Wave Superconductivity in Superconducting BaTi[2]Sb[2]O Revealed by [121/123]Sb-NMR/Nuclear Quadrupole Resonance Measurements
Author(s)	Kitagawa, S.; Ishida, K.; Nakano, Kousuke; Yajima, Takeshi; Kageyama, H.
Citation	Physical Review B (2013), 87(6)
Issue Date	2013-02-28
URL	http://hdl.handle.net/2433/187995
Right	©2013 American Physical Society
Type	Journal Article
Textversion	publisher

PHYSICAL REVIEW B **87**, 060510(R) (2013)

s-wave superconductivity in superconducting $BaTi_2Sb_2O$ revealed by $^{121/123}$Sb-NMR/nuclear quadrupole resonance measurements

S. Kitagawa,[1,*] K. Ishida,[1] K. Nakano,[2] T. Yajima,[2] and H. Kageyama[2]

[1]*Department of Physics, Graduate School of Science, Kyoto University, Kyoto 606-8502, Japan*

[2]*Department of Energy and Hydrocarbon Chemistry, Graduate School of Engineering, Kyoto University, Kyoto 615-8510, Japan*

(Received 25 September 2012; revised manuscript received 19 February 2013; published 28 February 2013)

We report the $^{121/123}$Sb-NMR/nuclear quadrupole resonance (NQR) measurements on the superconductor $BaTi_2Sb_2O$ with a two-dimensional Ti_2O square-net layer formed with Ti^{3+} ($3d^1$). NQR measurements revealed that the in-plane four-fold symmetry is broken at the Sb site below $T_A \sim 40$ K, without an internal field appearing at the Sb site. These exclude a spin-density wave (SDW)/ charge density wave (CDW) ordering with incommensurate correlations, but can be understood with the commensurate CDW ordering at T_A. The spin-lattice relaxation rate $1/T_1$, measured at the four-fold symmetry breaking site, decreases below superconducting (SC) transition temperature T_c, indicative of the microscopic coexistence of superconductivity and the CDW/SDW phase below T_A. Furthermore, $1/T_1$ of ^{121}Sb-NQR shows a coherence peak just below T_c and decreases exponentially at low temperatures. These results are in sharp contrast with those in cuprate and iron-based superconductors, and strongly suggest that its SC symmetry is classified to an ordinary *s*-wave state.

DOI: 10.1103/PhysRevB.87.060510 PACS number(s): 71.20.Be, 74.25.−q, 75.25.Dk, 76.60.−k

I. INTRODUCTION

After the discovery of high-T_c cuprate superconductors, many efforts have been made to synthesize new high-T_c superconductors. These activities have brought us the discovery of various unconventional superconductors, [e.g., Sr_2RuO_4,[1–3] $NaCoO_2{\cdot}1.5H_2O$,[4] and $LaFeAs(O_{1-x}F_x)$[5,6]] so far. It is quite interesting that all these superconductors possess a two-dimensional layered structure and are located near the magnetic instability, both of which are regarded as essential ingredients of high-T_c superconductors. Actually T_c in a quasi-two-dimensional system is theoretically shown to be higher than in a three-dimensional system, since magnetic fluctuation is generally enhanced by low dimensionality.[7]

Quite recently, it was reported that two-dimensional oxyantimonide $BaTi_2Sb_2O$ shows a superconducting (SC) transition at $T_c \sim 1$ K.[8,9] $BaTi_2Sb_2O$ possesses a similar crystal structure to cuprate La_2CuO_4 and has a Ti_2O square net, which is an anticonfiguration to the CuO_2 square net, as shown in Fig. 1. The edge-shared TiO_2Sb_4 octahedra form the square lattice, and the electronic state of Ti^{3+} is in the $3d^1$ state, which is regarded as an electron-hole symmetric state of $3d^9$ state in Cu^{2+}.[8] Thus, $BaTi_2Sb_2O$ is an interesting reference compound of cuprate superconductors although $BaTi_2Sb_2O$ is metallic. From the measurements of magnetic susceptibility and electrical resistivity, an anomaly was found at 50 K, and the occurrence of a charge density wave (CDW) or spin density wave (SDW) transition was suggested.[8,9] A similar anomaly was observed in ATi_2Pn_2O [$A = Na_2$, Ba, $(SrF)_2$, $(SmO)_2$; Pn = As, Sb] which have almost the same structure as $BaTi_2Sb_2O$ and show no superconductivity,[10–12] however details of this anomaly have not been investigated. Thus, the understanding of this anomaly, the electronic state of the Ti^{3+} ($3d^1$) and the SC symmetry are important for seeking another way for high-T_c superconductivity in the strong correlated 3*d* electron systems. In order to address the above underlying issues, we performed $^{121/123}$Sb-NMR/nuclear quadrupole resonance (NQR) measurements on $BaTi_2Sb_2O$.

II. EXPERIMENTAL

$BaTi_2Sb_2O$ was synthesized by the conventional solid state reaction method.[8] NMR measurements are performed in the same batch as magnetic susceptibility and resistivity measurements.[8] To prevent sample degradation by air and/or moisture, the polycrystalline sample was mixed with stycast 1266, and the mixture was solidified with random crystal orientation. All procedures were done in a glove box filled with N_2. $T_c \simeq 0.95$ K of the sample was determined from the diamagnetic shielding signal, which is consistent with the previous report.[8] No reaction was recognized between the sample and stycast, since T_c and T_A are unchanged during our measurements.

III. RESULTS AND DISCUSSION

Figure 2 shows the $^{121/123}$Sb-NQR spectra, which were obtained by frequency-swept method at 45 K ($>T_A$) and 4.2 K ($<T_A$). There are two isotopes of Sb nuclei, properties of which are summarized in Table I. When $I \geqslant 1$, a nucleus has an electric quadrupole moment Q as well as a magnetic dipole moment, and thus the degeneracy of nuclear-energy levels is lifted even at zero magnetic field due to the interaction between Q and the electric field gradient (EFG). This interaction is described as

$$\mathcal{H}_Q = \frac{\nu_{zz}}{6}\left\{\left(3I_z^2 - I^2\right) + \frac{1}{2}\eta\left(I_+^2 + I_-^2\right)\right\}, \qquad (1)$$

where ν_{zz} is the quadrupole frequency along the principal axis (*c* axis) of the EFG, and is defined as $\nu_{zz} \equiv 3e^2qQ/2I(2I-1)$ with $eq = V_{zz}$, and η is an asymmetry parameter of the EFG expressed as $(V_{xx} - V_{yy})/V_{zz}$ with $V_{\alpha\alpha}$, which is the EFG along the α direction ($\alpha = x, y, z,$). When ^{121}Sb (^{123}Sb) is in the presence of the EFG, the degenerate six (eight) nuclear-spin states are split into three (four) energy levels, yielding two (three) resonance frequencies as shown in Fig. 2. The quadrupole parameters ν_{zz} and η for each Sb nuclei are estimated from the comparison between the observed

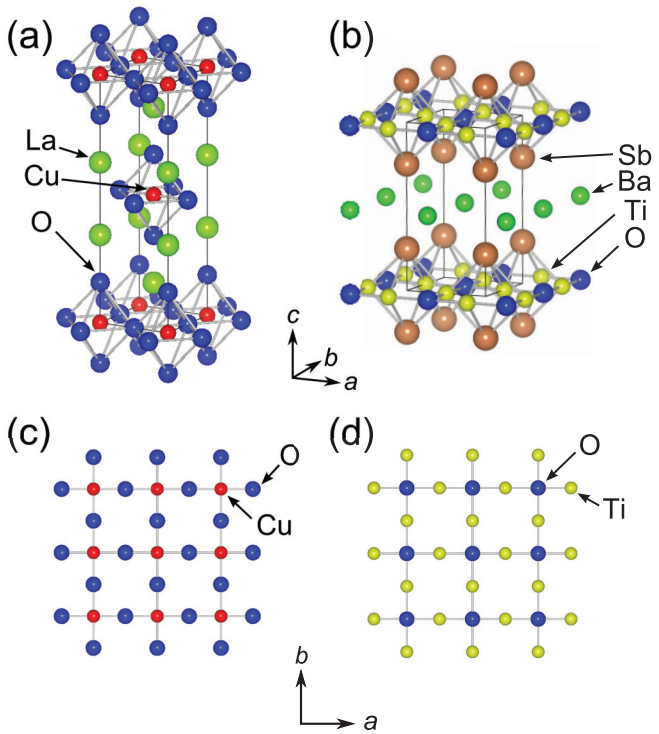

FIG. 1. (Color online) The crystal structure of (a) La_2CuO_4 and (b) $BaTi_2Sb_2O$. Both compounds possess a layer structure. (c) Two dimensional CuO_2 plane in La_2CuO_4, and (d) two-dimensional Ti_2O plane in $BaTi_2Sb_2O$.

$^{121/123}$Sb-NQR spectra and calculated resonance frequencies obtained from the diagonalization of Eq. (1) as shown in Fig. 2. Field-swept NMR spectra can be consistently fit by the simulation calculated with the same quadrupole parameters as shown in Fig. 4, indicative of the validity of the NQR analysis.

Reflecting the four-fold symmetry of the crystal structure, η is zero at 45 K, while the NQR spectrum is gradually shifted below 40 K. T dependence of the resonance frequencies arising from the $\pm 1/2 \leftrightarrow \pm 3/2$ (ν_1) and $\pm 3/2 \leftrightarrow \pm 5/2$ (ν_2) transition of ^{123}Sb is shown in Fig. 3(a). In the case of $I = 7/2$, NQR frequencies from each transition can be described as

$$\nu_1 = \nu_{zz}\left(1 + \frac{109}{30}\eta^2\right), \quad \text{and} \quad \nu_2 = 2\nu_{zz}\left(1 - \frac{17}{30}\eta^2\right)$$

within the second-order perturbation of η in $\mathcal{H}_Q$. Above 40 K, the experimental result shows the relation $\nu_2/\nu_1 \simeq 2(1 - \frac{21}{5}\eta^2) \simeq 2$ within the experimental error, but at 4.2 K, the result shows $\nu_2/\nu_1 \simeq 1.9$, which is evidence of finite η. From the above resonance frequencies, we derived T variation of η and ν_{zz}, which is shown in Fig. 3(b) and the inset, respectively. The T dependence of ν_{zz} is consistent with that in the lattice parameters,[8] indicative of the validity of the estimation. The spectra below T_A can be interpreted by the change of ν_{zz} and the finite η without an internal field appearing at the Sb site. This indicates the breaking of the in-plane four-fold symmetry at the Sb site at low temperatures. The η changes continuously below 40 K and no clear hysteresis is observed, showing the transition at T_A to be second order.

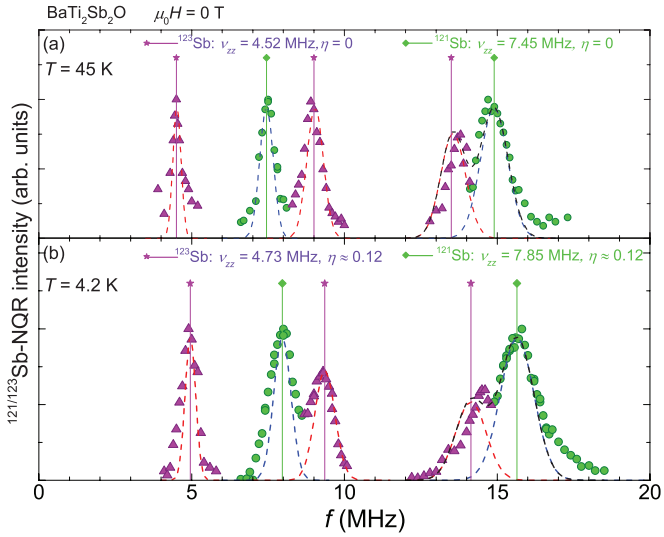

FIG. 2. (Color online) $^{121/123}$Sb-NQR spectra, which were obtained by frequency-swept method at (a) 45 K and (b) 4.2 K. From the observed $^{121/123}$Sb-NQR spectra, the quadrupole parameters for the Sb nuclei were evaluated as shown in the figure. The broken curves are the simulation of NQR spectra using the estimated quadrupole parameters. The asymmetry parameter η becomes finite at 4.2 K, indicative of the in-plane four-fold symmetry breaking at the Sb site. Linewidths of NQR spectra can be explained by only the electric field gradient distribution, indicative of the absence of internal magnetic field at the Sb site.

Next, we focus on the T dependence of low-energy spin dynamics probed with $1/T_1$ measurements at the Sb site. Figure 5 shows the T dependence of $1/T_1T$ of $^{121/123}$Sb-NQR in $BaTi_2Sb_2O$. Values of T_1 were derived by fitting the recovery data of $R(t) = 1 - m(t)/m(\infty)$ to the theoretical NQR recovery curves of $I = 5/2$ and $7/2$. Here $m(t)$ is the time dependence of spin-echo intensity at the peak of the NQR spectrum after saturation of nuclear magnetization, and $R(t)$ in the whole measurement range could be fit with a single component of T_1. $1/T_1T$ = const. (so-called "Korringa") behavior was observed above ~50 K, suggestive of the Fermi liquid (FL) state. Upon cooling, $1/T_1T$ starts to increase at 50 K, where the resistivity shows a kink, and exhibits a peak at around 40 K, followed by the FL state again upon further cooling. The constant value of $1/T_1T$ in a T range between 1.5 K and 10 K is ~1.1 ± 0.03, which is ~83% of $1/T_1T$ value above 50 K, indicative of the decrease of $N(E_F)$ by 9% below T_A, since $1/T_1T$ in the FL state is proportional to the square of the density of states (DOS) around the Fermi energy $N(E_F)$.

To investigate the origin of the phase transition, we measured $1/T_1T$ at two Sb isotopes and estimate $1/T_1$ ratio between the $^{121/123}$Sb isotopes ($^{121}T_1^{-1}/^{123}T_1^{-1}$) as shown in the

TABLE I. The data of Sb isotopes: the nuclear gyromagnetic ratio γ_n, the nuclear quadrupolar moment Q, natural abundance N.A., and the nuclear spin I.

	$\gamma_n/2\pi$ (MHz/T)	Q (10^{-24} cm^2)	N.A. (%)	I
^{121}Sb	10.189	$-0.2 \sim -1.8$	57.3	5/2
^{123}Sb	5.5175	$-0.2 \sim -0.7$	42.7	7/2

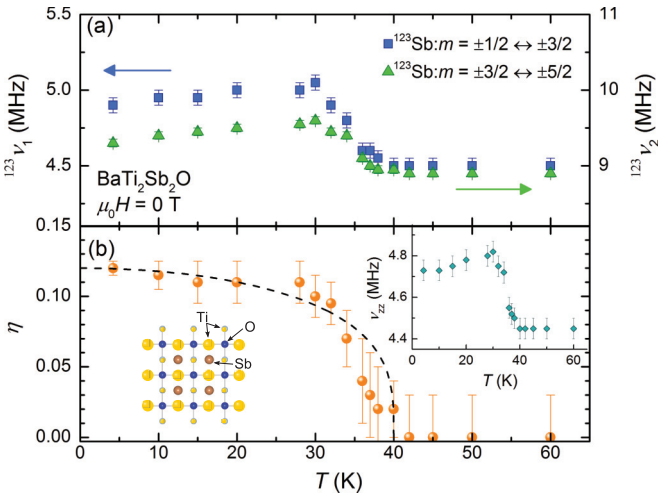

FIG. 3. (Color online) T dependence of (a) resonance frequencies of $\pm1/2 \leftrightarrow \pm3/2$ (ν_1) and $\pm3/2 \leftrightarrow \pm5/2$ (ν_2) transition of ^{123}Sb and (b) η. The quadrupole parameters ν_{zz} and η are estimated from these resonance frequencies. The η changes continuously below $\simeq$40 K and no appreciable hysteresis is observed, indicating that this phase transition is second order. The broken line is a guide to the eyes. The schematic image of the CDW state, which is one of the promising states below T_A, is illustrated, where the difference of the circle size at the Ti site represents the difference of the charge densities of Ti. (Inset) T dependence of ν_{zz}. The variation in ν_{zz} is consistent with that in lattice parameters, indicative of the validity of the NQR analysis.

inset of Fig. 5. In general, an NMR/NQR spin lattice relaxation occurs through magnetic and/or electric-quadrupole channels. In the case of magnetic channel, fluctuations of local magnetic fields at a nuclear site cause magnetic relaxations between the nuclear spin levels of $\Delta m = \pm1$. The magnetic relaxation rate is related to the gyromagnetic ratio γ_n by $T_{1M}^{-1} \propto \gamma_n^2$. Therefore,

$$\frac{^{121}T_{1M}^{-1}}{^{123}T_{1M}^{-1}} = \left(\frac{10.189}{5.5175}\right)^2 = 3.41$$

is estimated from Table I.

On the other hand, fluctuations of EFG cause electric quadrupole relaxation between the nuclear spin levels of $\Delta m = \pm1$ and $\Delta m = \pm2$. In this case, the electric-quadrupole relaxation rate is related to the quadrupole moment Q by $T_{1Q}^{-1} \propto 3(2I+3)Q^2/[10(2I-1)I^2]$.[13] From obtained $\nu_{zz} \equiv 3e^2qQ/2I(2I-1)$, the ratio of $^{121}Q/^{123}Q$ can be estimated as

$$\frac{^{121}Q}{^{123}Q} = \frac{\frac{2}{3}\cdot\frac{5}{2}(2\cdot\frac{5}{2}-1)\cdot{}^{121}\nu_{zz}}{\frac{2}{3}\cdot\frac{7}{2}(2\cdot\frac{7}{2}-1)\cdot{}^{123}\nu_{zz}} \simeq 0.80.$$

Then,

$$\frac{^{121}T_{1Q}^{-1}}{^{123}T_{1Q}^{-1}} = \frac{\frac{3(2\cdot\frac{5}{2}+3)}{10(2\cdot\frac{5}{2}-1)(\frac{5}{2})^2}}{\frac{3(2\cdot\frac{7}{2}+3)}{10(2\cdot\frac{7}{2}-1)(\frac{7}{2})^2}}\left(\frac{^{121}Q}{^{123}Q}\right)^2 \simeq 2.34\times0.80^2 = 1.50$$

is calculated. From the NQR measurements, the ratio of $^{121}T_1^{-1}/^{123}T_1^{-1}$ is $\sim$3, indicating that the magnetic relaxation process is dominated in the whole temperature range and magnetic fluctuations enhance toward $\simeq$40 K.

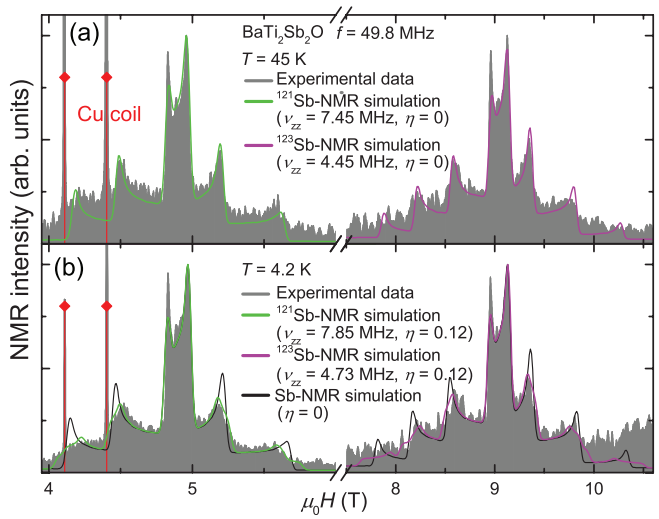

FIG. 4. (Color online) Field-swept $^{121/123}$Sb-NMR spectra measured at 45 K (a) and 4.2 K (b) measured at 49.8 MHz. Simulations of NMR spectra calculated with the same NQR parameter as NQR spectra are also shown. The measured NMR spectra can be consistently reproduced by the simulation, showing the validity of the NQR analysis. For comparison, simulations of NMR spectra with $\eta = 0$ are shown at $T = 4.2$ K.

Here we discuss the origin of the anomaly at T_A on the basis of experimental results reported so far. As mentioned above, a CDW /SDW ordering accompanied with the anomaly in the lattice parameters was suggested from the resistivity and susceptibility measurements, although a tetragonality is maintained below T_A.[8,14] On the other hand,

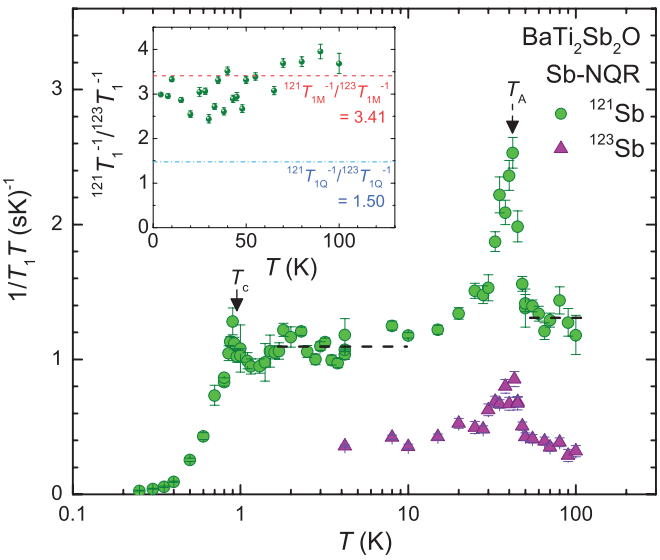

FIG. 5. (Color online) T dependence of $1/T_1T$ measured with $^{121/123}$Sb-NQR. $1/T_1T$ is constant above 60 K, suggestive of the conventional Fermi liquid (FL) state. Upon cooling, $1/T_1T$ shows a peak at $T_A \sim 40$ K. Upon further cooling, $1/T_1T$ recovers the FL state below 10 K with slightly smaller values than those above 50 K. (Inset) T dependence of the $^{121/123}$Sb isotopic ratio $^{121}T_1^{-1}/^{123}T_1^{-1}$. $^{121}T_1^{-1}/^{123}T_1^{-1} \sim 3$, indicating that the magnetic process is dominant in the whole temperature range.

the $^{121/123}$Sb-NMR/NQR spectra at low temperatures revealed that the in-plane four-fold symmetry is broken at the Sb site below $T_A \sim 40$ K without the internal field appearing at the Sb site. The absence of an internal field excludes the SDW ordering with an incommensurate correlation, since otherwise internal fields should appear at the Sb site, resulting in resonance peaks, particularly those arising from the transition between $m = \pm 1/2$ and $\pm 3/2$, that are split or broadened.

Alternatively, the change of the NQR spectra below T_A can be understood by the occurrence of the commensurate CDW ordering. When a CDW transition occurs, there appear several Ti sites with different charge densities in most cases. However, the shift of the $^{121/123}$Sb NQR peak without splitting nor appreciable broadening below T_A gives a strong constraint and indicates that charge densities at the Ti sites should have a commensurate correlation, since there would be several Sb sites induced below T_A if a CDW ordering possesses an incommensurate correlation. The different charge densities at the Ti sites, e.g., the Ti configuration shown in Fig. 3(b), break the in-plane four-fold symmetry at the Sb site although a tetragonality is maintained below T_A. The charge difference at the Ti site is considered to be small since the change of the DOS probed with $1/T_1T$ and the kink of the resistivity are very small below T_A. However, the possibility of the magnetic ordering together with the CDW ordering at T_A would not be ruled out, since we cannot exclude commensurate magnetic ordering with a specific relationship between magnetic correlations and ordered moment direction [e.g., internal fields are canceled out at the Sb site when magnetic correlations are checkerboard (π,π) and ordered moments direct to the c axis, even if the off-diagonal hyperfine fields are taken into account[15,16]]. To exclude the possibility of magnetic ordering, NMR/NQR measurements at the Ti site and/or neutron scattering measurements are crucial. It should be noted that magnetic fluctuations are enhanced toward T_A. In a well-known $2H$-$NbSe_2$, where superconductivity ($T_c \sim 7$ K) occurs below the CDW transition at $T_{CDW} \sim 35$ K, no anomaly was observed in $1/T_1$ at T_{CDW},[17] however the similar anomaly of $1/T_1$ as in $BaTi_2Sb_2O$ was observed in $Lu_5Ir_4Si_{10}$ at T_{CDW}.[18] Since the relationship between charge and magnetic degree of freedom has not been well understood, $BaTi_2Sb_2O$ might be one of the suitable systems to investigate a correlation between charge and spin dynamics.

Next, we discuss the $1/T_1$ in the SC state. $1/T_1$ of ^{121}Sb-NQR slightly decreases below 1.5 K, where a small Meissner signal appears, but $1/T_1$ shows a tiny coherence peak just below $T_c \simeq 0.95$ K, where the sharp Meissner signal is observed, and then rapidly decreases at low temperatures as shown in Fig. 6. T dependence of $1/T_1$ far below T_c is much steeper than T^3 dependence, but T_1 follows an exponential T dependence down to 0.3 K, as shown by an Arrhenius plot in the inset of (b). These are in sharp contrast with T dependence in cuprate[19] and iron-based superconductors.[6] From the slope of the plot, the magnitude of the SC gap is estimated to be $2\Delta/k_BT_c = 4.4$, and actually the observed $1/T_1$ in the SC state can be fit consistently by an s-wave full gap model with $2\Delta/k_BT_c = 4.4$ and $\delta/\Delta = 0.5$, where δ is the broadening parameter of the singularity in the SC DOS. Absence of the residual DOS in the SC state is also consistent with an s-wave model, since residual DOS suggested by the Korringa behavior far below T_c is easily introduced by disorder and/or a tiny amount of impurities in unconventional superconductors.[20,21] Since the present NQR measurements were done in an "early-stage" polycrystalline sample, the full-gap s-wave state would be the most possible SC gap state in $BaTi_2Sb_2O$.

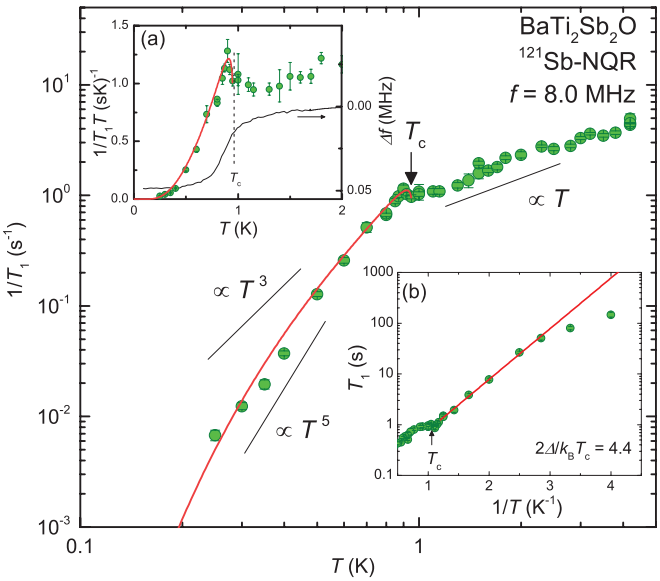

FIG. 6. (Color online) T dependence of $1/T_1$ measured at 8.0 MHz. The inset of (a) shows the T dependence of $1/T_1T$ and a diamagnetic shielding signal measured by an NMR coil around T_c, and the inset of (b) shows the Arrhenius plot of T_1. As seen in the insets of (a) and (b), $1/T_1$ shows a coherence peak just below $T_c \simeq 0.95$ K and rapidly decreases at low temperatures. The red curves are a calculation of T dependence of $1/T_1$ based on an s-wave model with a finite gap. In the s-wave model, $2\Delta/k_BT_c = 4.4$ and $\delta/\Delta = 0.5$ are adopted, where δ/Δ are the broadening parameter of the SC gap. $1/T_1$ results in the SC state are consistently reproduced with the s-wave model.

IV. SUMMARY

In summary, the NQR asymmetric parameter η becomes finite below $T_A \simeq 40$ K, indicative of the breaking of the in-plane four-fold symmetry at the Sb site without an internal field appearing at the Sb site. The variation of the NQR spectra below T_A can be understood by the occurrence of the commensurate CDW transition. $1/T_1$ below T_A shows a further anomaly below T_c due to the opening of the SC gap, indicative of the coexistence of superconductivity and the anomaly occurring at T_A. In the SC state, $1/T_1$ shows a coherence peak just below T_c and exponentially decreases at low temperatures, which strongly suggests that the SC symmetry of $BaTi_2Sb_2O$ is an s wave with finite SC gap.

ACKNOWLEDGMENTS

The authors thank Y. Nakai, K. Kitagawa, S. Yonezawa, and Y. Maeno for experimental support and valuable discussions. The authors are also grateful to T. Tohyama for fruitful

discussions. This work was partially supported by Kyoto Univ. LTM center, the "Heavy Electrons" Grant-in-Aid for Scientific Research on Innovative Areas (No. 20102006) from The Ministry of Education, Culture, Sports, Science, and Technology (MEXT) of Japan, a Grant-in-Aid for the Global COE Program "The Next Generation of Physics, Spun from Universality and Emergence" from MEXT of Japan, a Grant-in-aid for Scientific Research from Japan Society for Promotion of Science (JSPS), KAKENHI (S and A) (No. 20224008 and No. 23244075), and FIRST program from JSPS. One of the authors (S.K.) is financially supported by a JSPS Research Fellowship.

*shunsaku@scphys.kyoto-u.ac.jp

[1] Y. Maeno, H. Hashimoto, K. Yoshida, S. Nishizaki, T. Fujita, J. G. Bednorz, and F. Lichthnberg, Nature (London) **372**, 532 (1994).

[2] A. P. Mackenzie and Y. Maeno, Rev. Mod. Phys. **75**, 657 (2003).

[3] Y. Maeno, S. Kittaka, T. Nomura, S. Yonezawa, and K. Ishida, J. Phys. Soc. Jpn. **81**, 011009 (2012).

[4] K. Takada, H. Sakurai, E. Takayama-Muromachi, F. Izumi, R. A. Dilanian, and T. Sasaki, Nature (London) **422**, 53 (2003).

[5] Y. Kamihara, T. Watanabe, M. Hirano, and H. Hosono, J. Am. Chem. Soc. **130**, 3296 (2008).

[6] K. Ishida, Y. Nakai, and H. Hosono, J. Phys. Soc. Jpn. **78**, 062001 (2009).

[7] Y. Yanase, T. Jujo, T. Nomura, H. Ikeda, T. Hotta, and K. Yamada, Phys. Rep. **387**, 1 (2003).

[8] T. Yajima, K. Nakano, F. Takeiri, T. Ono, Y. Hosokoshi, Y. Matsushita, J. Hester, Y. Kobayashi, and H. Kageyama, J. Phys. Soc. Jpn. **81**, 103706 (2012).

[9] P. Doan, M. Gooch, Z. Tang, B. Lorenz, A. Moeller, J. Tapp, P. C. W. Chu, and A. M. Guloy, J. Am. Chem. Soc. **134**, 16520 (2012).

[10] E. A. A. III, T. Ozawa, S. M. Kauzlarich, and R. R. Singh, J. Solid State Chem. **134**, 423 (1997).

[11] X. F. Wang, Y. J. Yan, J. J. Ying, Q. J. Li, M. Zhang, N. Xu, and X. H. Chen, J. Phys.: Condens. Matter **22**, 1503 (2010).

[12] R. H. Liu, Y. A. Song, Q. J. Li, J. J. Ying, Y. J. Yan, Y. He, and X. H. Chen, Chem. Mater. **22**, 1503 (2010).

[13] Y. Obata, J. Phys. Soc. Jpn. **19**, 2348 (1964).

[14] T. C. Ozawa, R. Pantoja, E. A. A. III, S. M. Kauzlarich, J. E. Greedan, M. Bieringer, and J. W. R., Jr., J. Solid State Chem. **153**, 275 (2000).

[15] K. Kitagawa, N. Katayama, K. Ohgushi, M. Yoshida, and M. Takigawa, J. Phys. Soc. Jpn. **77**, 114709 (2008).

[16] S. Kitagawa, Y. Nakai, T. Iye, K. Ishida, Y. Kamihara, M. Hirano, and H. Hosono, Phys. Rev. B **81**, 212502 (2010).

[17] K. Ishida, Y. Niino, G.-Q. Zheng, Y. Kitaoka, K. Asayama, and T. Ohtani, J. Phys. Soc. Jpn. **65**, 2341 (1996).

[18] Y. Nakazawa, presented at the 58th JPS annual meeting, 29aPS (2003).

[19] K. Ishida, Y. Kitaoka, T. Yoshitomi, N. Ogata, T. Kamino, and K. Asayama, Physica C **179**, 29 (1991).

[20] Y. Nakai, T. Iye, S. Kitagawa, K. Ishida, S. Kasahara, T. Shibauchi, Y. Matsuda, and T. Terashima, Phys. Rev. B **81**, 020503(R) (2010).

[21] K. Ishida, Y. Kitaoka, K. Asayama, S. Ikeda, S. Nishizaki, Y. Maeno, K. Yoshida, and T. Fujita, Phys. Rev. B **56**, R505 (1997).